

AD-A058 572

AEROSPACE CORP EL SEGUNDO CALIF IVAN A GETTING LABS F/G 4/1
LOW ALTITUDE MEASUREMENTS OF PRECIPITATING PROTONS, ALPHA PARTI--ETC(U)
AUG 78 M SCHOLER, D HOVESTADT, G HARTMANN F04701-77-C-0078

UNCLASSIFIED

TR-0078(3960-05)-12

SAMSO-TR-78-80

NL

1 OF 1
AD
A058 572



LEVEL II

12
NW

Low Altitude Measurements of Precipitating Protons, Alpha Particles, and Heavy Ions During the Geomagnetic Storm of 26-27 March 1976

AD A058572

UJ No. _____
JDC FILE COPY

M. SCHOLER, D. HOVESTADT, and G. HARTMANN
Institut fur Extraterrestrische Physik,
Max-Planck Institut fur Physik and Astrophysik
J. B. BLAKE and J. F. FENNELL
Space Sciences Laboratory
The Ivan A. Getting Laboratories
The Aerospace Corporation
El Segundo, Calif. 90245
and
G. GLOECKLER
Department of Astronomy
University of Maryland

15 August 1978

Interim Report

APPROVED FOR PUBLIC RELEASE;
DISTRIBUTION UNLIMITED



Prepared for
SPACE AND MISSILE SYSTEMS ORGANIZATION
AIR FORCE SYSTEMS COMMAND
Los Angeles Air Force Station
P.O. Box 92960, Worldway Postal Center
Los Angeles, Calif. 90009

78 09 07 020

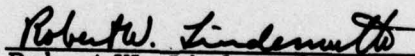
This interim report was submitted by The Aerospace Corporation, El Segundo, CA 90245, under Contract No. F04701-77-C-0078 with the Space and Missile Systems Organization, Deputy for Advanced Space Programs, P.O. Box 92960, Worldway Postal Center, Los Angeles, CA 90009. It was reviewed and approved for The Aerospace Corporation by G. A. Paulikas, Director, Space Sciences Laboratory. Lieutenant A. G. Fernandez, SAMSO/YCPT, was the project officer for Advanced Space Program.

This report has been reviewed by the Information Office (OI) and is releasable to the National Technical Information Service (NTIS). At NTIS, it will be available to the general public, including foreign nations.

This technical report has been reviewed and is approved for publication. Publication of this report does not constitute Air Force approval of the report's findings or conclusions. It is published only for the exchange and stimulation of ideas.



Arturo G. Fernandez, Lt, USAF
Project Officer



Robert W. Lindemuth, Lt Col, USAF
Chief, Technology Plans Division

FOR THE COMMANDER



FLOYD R. STUART, Col, USAF
Deputy for Advanced Space Programs

UNCLASSIFIED

SECURITY CLASSIFICATION OF THIS PAGE (When Data Entered)

REPORT DOCUMENTATION PAGE		READ INSTRUCTIONS BEFORE COMPLETING FORM
1. REPORT NUMBER SAMS0-TR-78-80	2. GOVT ACCESSION NO.	3. RECIPIENT'S CATALOG NUMBER
4. TITLE (and Subtitle) LOW ALTITUDE MEASUREMENTS OF PRECIPITATING PROTONS, ALPHA PAR- TICLES, AND HEAVY IONS DURING THE GEOMAGNETIC STORM OF 26-27 MARCH 1978		5. TYPE OF REPORT & PERIOD COVERED Interim RPTs
6. AUTHOR(s) Manfred Scholer, Dieter Hovestadt, Gerhard Hartmann, J. Bernard Blake, Joseph F. Fennell, George Gloeckler		7. PERFORMING ORG. REPORT NUMBER TR-0078(3960-05)-12
8. PERFORMING ORGANIZATION NAME AND ADDRESS The Aerospace Corporation El Segundo, Calif. 90245		9. CONTRACT OR GRANT NUMBER(s) F04701-77-C-0078
10. CONTROLLING OFFICE NAME AND ADDRESS Space and Missile Systems Organization Air Force Systems Command Los Angeles, Calif. 90009		11. PROGRAM ELEMENT, PROJECT, TASK AREA & WORK UNIT NUMBERS
12. MONITORING AGENCY NAME & ADDRESS (if different from Controlling Office)		13. REPORT DATE 15 August 1978
14. DISTRIBUTION STATEMENT (of this Report) Approved for public release; distribution unlimited.		15. NUMBER OF PAGES 32
16. DISTRIBUTION STATEMENT (of the abstract entered in Block 20, if different from Report)		17. SECURITY CLASS. (of this report) Unclassified
18. SUPPLEMENTARY NOTES		19. DECLASSIFICATION/DOWNGRADING SCHEDULE
19. KEY WORDS (Continue on reverse side if necessary and identify by block number) Heavy Ions Precipitating Ions Magnetic Storm		
20. ABSTRACT (Continue on reverse side if necessary and identify by block number) During the geomagnetic storm of 26 March 1976, observations were made of precipitating protons, alpha particles, and heavy ions by two counter tele- scopes aboard the low-altitude S3-2 satellite. These observations are pre- sented in this paper and their significance discussed. Briefly, a two zone precipitation region is observed on the night side, at $L \approx 2.7$ and $L \approx 4.0$ with an α/p ratio $\sim 8 \times 10^{-3}$ in the low latitude region and $\sim 9 \times 10^{-4}$ at higher latitude at 0.4 MeV/nucleon. The heavier ions, CNO nuclei, are seen in the low latitude zone with a CNO/ α ratio of $\sim 5.6 \times 10^{-2}$ at 0.25 MeV/nucleon.		

DD FORM 1473
(FACSIMILE)

UNCLASSIFIED

SECURITY CLASSIFICATION OF THIS PAGE (When Data Entered)

409 944

PREFACE

The design, construction, and integration of the instruments was the work of several people. The authors would like to acknowledge the substantial efforts of Erick Kunneth and Otto Vollmer of the Max-Planck-Institut, Norm Katz and Sam Imamoto of The Aerospace Corporation, and Ed Tums and John Cain of the University of Maryland.

ACCESSION for	
NTIS	Write Section <input checked="checked" type="checkbox"/>
DDC	Buff Section <input type="checkbox"/>
UNANNOUNCED	<input type="checkbox"/>
JUSTIFICATION _____	
BY _____	
DISTRIBUTION/ANNUALITY NOTES	
DI	SPECIAL
A	

blank
2

CONTENTS

PREFACE	1
INTRODUCTION	7
SATELLITE AND INSTRUMENTATION	9
OBSERVATIONS	11
SUMMARY OF OBSERVATIONS	27
DISCUSSION	29
REFERENCES	31

blank
4

TABLE

1.	Sensor Parameters	21
----	-------------------------	----

FIGURES

1.	Precipitation Zones of Alpha Particles and Heavy Ions as Function UT	14
2.	Proton, Alpha Particle, and Heavy Ion Countrates for (a) Pre-Storm Pass, and (b) Dayside Pass at End of Storm Main Phase	15
3.	Proton, Alpha Particle, and Heavy Ion Countrates for Two Nightside Passes at the End of the Storm Main Phase	16
4.	Proton, Alpha Particle, and Heavy Ion Countrates for (a) Nightside Pass, and (b) Dayside Pass in Storm Recovery Phase	17
5.	Pitch Angle Distributions of Protons and Alpha Particles on 26 March 1976	19
6.	Proton and Alpha Particle Differential Spectra Parallel to the Magnetic Field (upward) at $L = 2.59$ on 26 March 1976 at 0855 UT	22
7.	Proton and Alpha Particle Differential Spectra in the Precipitation Event at $L = 2.7$ on 26 Mary 1976 at 0856 UT	23
8.	Proton and Alpha Particle Differential Spectra in the High Latitude Precipitation Zone at $L = 4.8$ on 27 March 1976 at 1649 UT	25

b/gnk

INTRODUCTION

Detailed low altitude measurements of precipitating protons at energies above 100 keV, and at lower, ring current energies have been reported by a number of authors (e.g., Amundsen et al., 1972; Mizera, 1974; S  raas and Berg, 1974; Hauge and S  raas, 1975; S  raas et al., 1977). From these measurements the following picture has emerged: During geomagnetically quiet conditions there exists at high latitudes in the evening-midnight sector a region where the protons have a roughly isotropic pitch angle distribution. Equatorward of the isotropic region there is a latitude interval where the pitch angle distribution is anisotropic (with no particles in the loss cone). At still lower latitudes there appear again protons in the loss cone, indicating weak to moderate pitch angle diffusion. During geomagnetically disturbed times the equatorward boundary of the isotropic region moves to lower latitudes and has been observed as low as $L = 3$ (Lindalen and Egeland, 1972).

Low altitude measurements reveal only a small part of the equatorial pitch angle distribution. However, near equatorial measurements of energetic protons on the Explorer 45 (S^3) satellite by Williams and Lyons (1974a, 1974b) confirm the picture described above. During the geomagnetic storm recovery phase they observed isotropic pitch angle distributions with a nearly empty loss cone above the plasmapause region. In the region of the plasmapause they observed a transition from flat to rounded pitch angle distributions, indicating weak pitch angle scattering. Apogee of Explorer 45 was not high enough to observe the outer region of strong turbulence except during the geomagnetic storm main phase when this region moves to lower altitudes. During one geomagnetic storm Williams and Lyons (1974b) reported observations of flat pitch angle distributions with a full loss cone in the storm main phase at $L \approx 4.2$.

In this report we present observational data on precipitating protons which confirm these earlier results and, for the first time, data on precipitating alpha particles and heavy ions with $Z > 4$. Composition measurements of energetic particles in the magnetosphere are still rare (for recent reviews see, e.g., Fennell and Blake, 1976; Fritz, 1976), and new data on this subject should provide additional insight into the origin and dynamics of magnetospheric particles.

SATELLITE AND INSTRUMENTATION

The data presented in this paper were obtained from a proton and a heavy ion telescope on board the polar orbiting S3-2 satellite (inclination 96.3° , perigee ~ 230 km, apogee ~ 1500 km). The satellite is spin-stabilized with the spin axis maintained normal to the orbital plane; the spin period is 18.8 seconds. The two instruments are mounted with their apertures orthogonal to the spin axis.

Because of the large differences of proton, alpha particle and heavy ion fluxes in the radiation belt, the dynamical range required to measure all ion species simultaneously with reasonable statistical significance could not be achieved with a single detector system. Therefore two different instruments were employed.

The proton spectrometer uses a single silicon semiconductor detector of $200\text{ }\mu\text{m}$ thickness for energy analysis, followed by a solid state anticoincidence detector. The particle acceptance angle is limited to 18° full angle, resulting in a geometrical factor of 0.04 cm^2 ster. The 5 integral proton channels p1 to p5 and the one integral alpha channel $\alpha 0$ are listed in Table 1.

The alpha particle and heavy ion telescope is similar to the ULET instrument of the University of Maryland/Max-Planck-Institute experiment on IMP 7 and IMP 8 (Hovestadt and Vollmer, 1971). The telescope is a three detector device. The first detector is a thin proportional counter filled with $125\text{ }\mu\text{g/cm}^2$ of isobutane. In this detector the specific energy loss ΔE of the penetrating particle is measured. The residual energy E is deposited in the second detector, a silicon semiconductor of $800\text{ }\mu\text{m}$ thickness. Particles penetrating the second detector, are rejected by an anticoincidence

detector. The field-of-view is 49° full angle; the geometric factor is $0.52 \text{ cm}^2 \text{ ster}$. This telescope provides a unique identification of protons, alpha particles and heavy ions ($Z > 4$ and $Z > 16$). The effective threshold for both C and O in the $Z > 4$ channel is $\approx 0.25 \text{ MeV/nucleon}$. The channels are listed in Table 1. All channels are read out once per sec, except for the proton channels pi1 and pi2, the alpha particle channel $\alpha 6$ and the single rates in the three detectors. The latter channels are multiplexed in an 8-channel multiplexer with a 1 sec simultaneous accumulation time. A randomly selected sample of the heavy ion events is pulse height (2D) analyzed with up to 3 analyses per sec.

Because of the large geometrical factor of the ion telescope, the proton channels pi1 and pi2 saturate when passing through the outer radiation belt. Therefore, these channels are used only for a consistency check with the proton telescope measurements in regions of space where suitable fluxes were encountered. These checks reveal an excellent agreement of the proton fluxes measured by the two different systems. The saturation effects mentioned above occur in the proton logic and not in the detectors, amplifiers or discriminators; the saturation effects do not impair the heavy ion channels.

The alpha particle channels $\alpha 1$ to $\alpha 6$ consist of two groups with different thresholds in the ΔE signal. The low energy channels $\alpha 1$ to $\alpha 3$ have a ΔE -threshold 5.6 times higher than the ΔE -threshold utilized in the high energy channels $\alpha 4$ to $\alpha 6$. Where the proton single rates are very high in the radiation belts, some chance coincidence and pile-up effects contaminate the alpha particle channel $\alpha 4$. Only $\alpha 4$ is affected.

The excellent background rejection capability of the ion telescope is demonstrated by the following: In the inner radiation belt the $\alpha 1$ rate is $< 1 \text{ count/sec}$ in spite of the high singles rates in the ΔE and E channels of $\sim 5 \times 10^4/\text{sec}$ and $\sim 10^5/\text{sec}$, respectively.

In this paper we use only the rates with high ΔE thresholds. The $Z > 4$ channel has a ΔE threshold of 4.5 times the $\alpha 1$ to $\alpha 3$ thresholds and is therefore even less sensitive to pile-up and chance coincidence background than $\alpha 1$ to $\alpha 3$.

blank
12

OBSERVATIONS

The data presented in this paper cover the period March 24-28, 1976. A large geomagnetic storm ($D_{st} = -230\gamma$) and an energetic solar particle event occurred within this time period. The top panel of Figure 1 shows the D_{st} value; the bars in the top panel indicate the time intervals of data retrieval.

The large geomagnetic storm occurred after the SSC on March 25, 2339 UT. The D_{st} index remained quiet until ~ 0200 UT on March 26, then started to decrease suddenly and reached -230γ at 0800 UT. Thereafter the D_{st} index slowly recovered to reach -80γ to -90γ on March 28, 1976. In the following, we will investigate the time development of fluxes and pitch angle distributions of protons, alpha particles, and heavy ions measured at low altitudes during the formation and decay of the equatorial ring current. Examples of the particle measurements during various satellite passes are shown in Figures 2 to 4.

Figure 2a is an example of the fluxes measured during a pre-storm crossing of the outer radiation belt. The pitch angle distributions are strongly peaked at 90° to the geomagnetic field. The alpha particle and proton channels of the two instruments do not cover the identical energy per nucleon range. In order to determine the α/p ratios at the same energy per nucleon we have adopted the following procedure: The measured fluxes in adjacent channels are connected by power laws. The spectral exponents and the absolute intensities are determined by the fact that the integrals over the power laws between the channel boundaries must be equal to the measured fluxes. From the power laws we then derive α/p ratios at different energy per nucleon values. During the pre-storm quiet time we find at $L = 3.87$, $B = 0.307$ G that the α/p ratios (perpendicular to the geomagnetic field) are $\sim 1.2 \times 10^{-3}$, 6.1×10^{-4} and 3.3×10^{-4} at 0.4, 0.5, and 0.6 meV/nucleon, respectively.

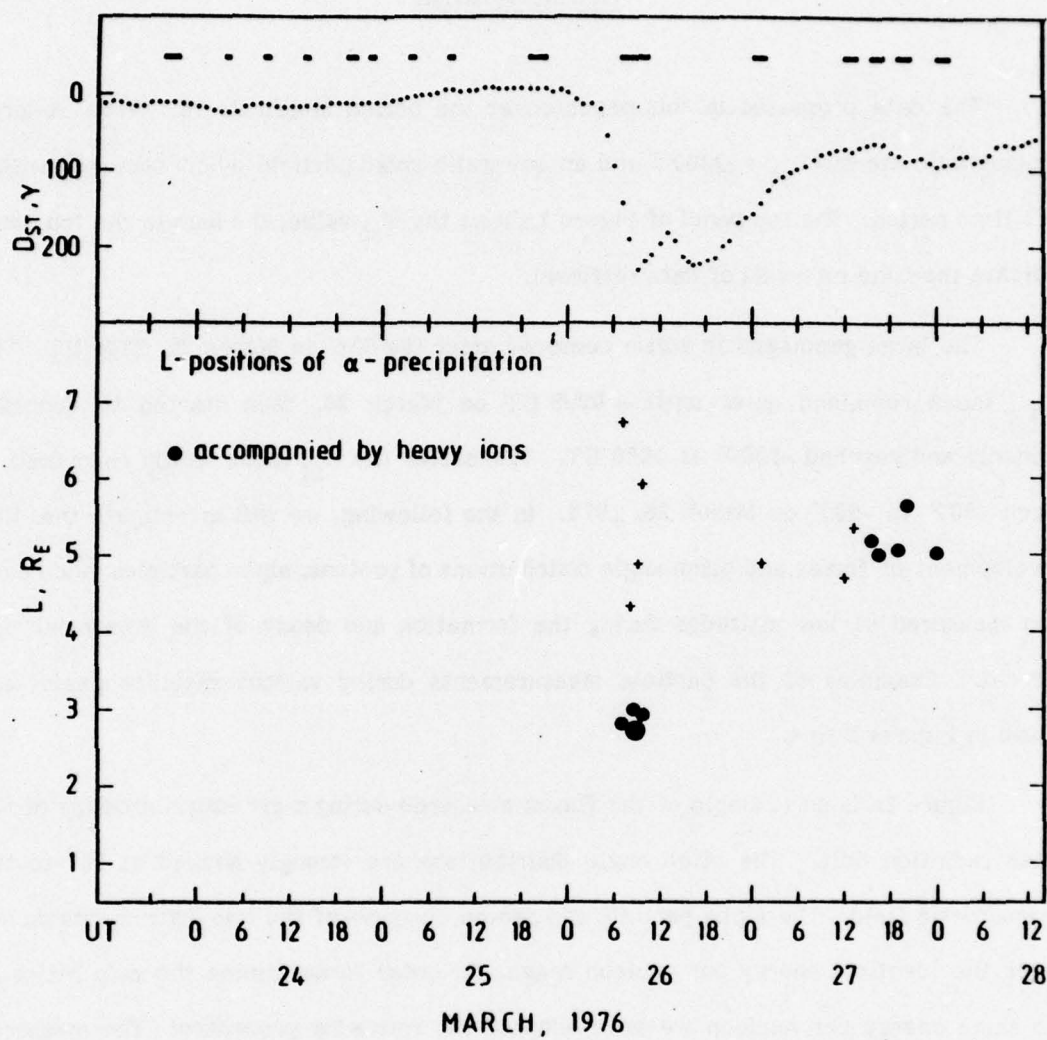


Fig. 1. Precipitation Zones of Alpha Particles and Heavy Ions as Function of UT. The value of D_{st} as a function of UT is also shown.

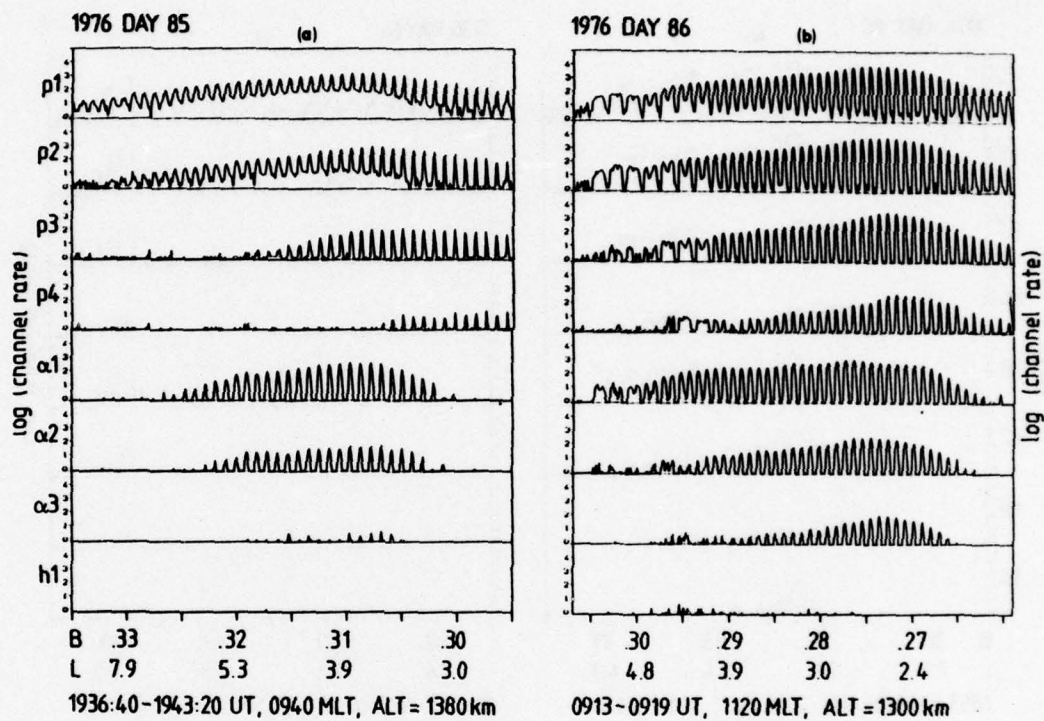


Fig. 2. Proton, Alpha Particle, and Heavy Ion Count rates for (a) Pre-Storm Pass, and (b) Dayside Pass at End of Storm Main Phase

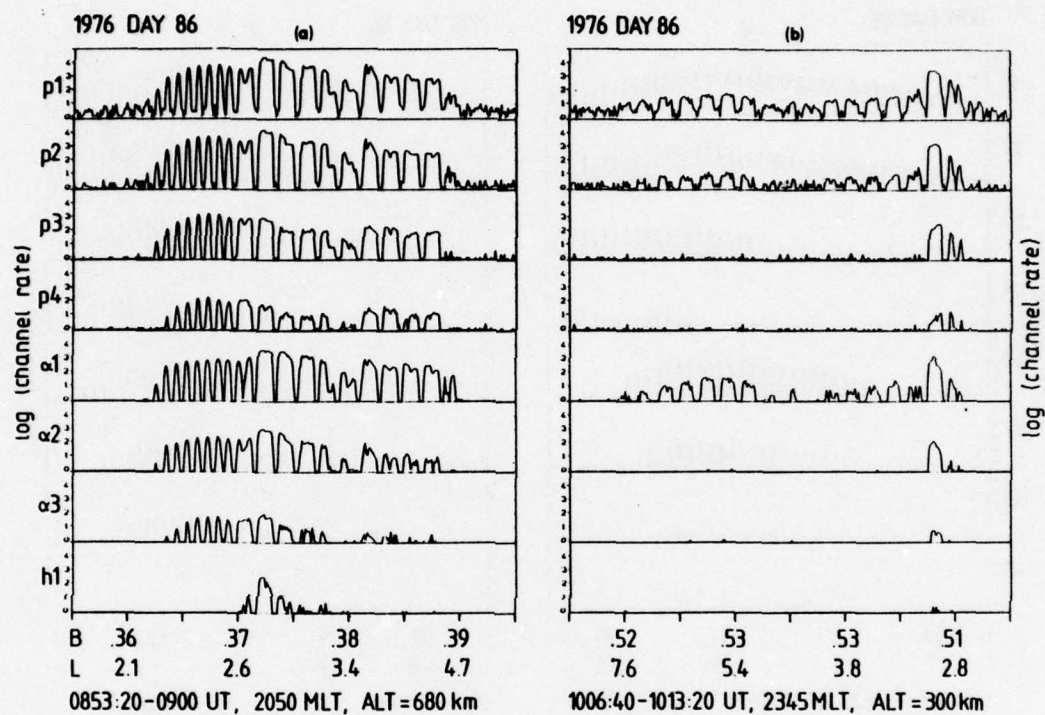


Fig. 3. Proton, Alpha Particle, and Heavy Ion Count rates for Two Nightside Passes at the End of the Storm Main Phase

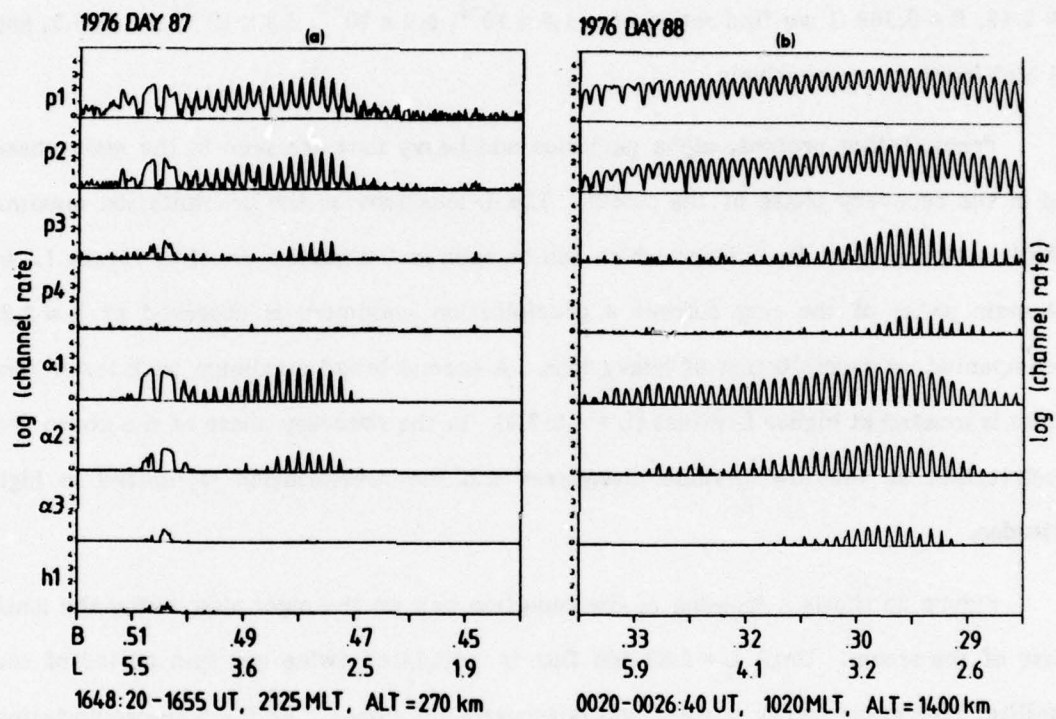


Fig. 4. Proton, Alpha Particle, and Heavy Ion Count rates for (a) Nightside Pass, and (b) Dayside Pass in Storm Recovery Phase

With the formation of the ring current, the L-location of the flux maximum of the trapped alpha particles moves to slightly lower L-values, the absolute fluxes increase considerably and the α/p ratio perpendicular to the geomagnetic field is enhanced. At $L = 2.48$, $B = 0.368$ G we find ratios of $\sim 1.8 \times 10^{-2}$, 5.9×10^{-3} , 2.3×10^{-3} at 0.4, 0.5, and 0.6 MeV/nucleon, respectively.

Precipitating protons, alpha particles and heavy ions are seen in the main phase and in the recovery phase of the storm. The L-locations of the precipitation maxima exhibit a strong time dependence which can be seen in the bottom panel of Figure 1. In the main phase of the ring current a precipitation maximum is observed at $L \approx 2.8$, accompanied by precipitation of heavy ions. A second broad maximum with lower flux values is located at higher L-values ($L = 4.5-7.0$). In the recovery phase of the storm the precipitation at the low L-value disappears and the precipitation is limited to high latitudes.

Figure 3a shows a crossing of the radiation belt on the night side during the main phase of the storm. Until $L = 2.53$ the flux is modulated twice per spin period of the satellite, indicating empty upward and downward loss cones. At $L = 2.59$ precipitating particles can be seen in the upper loss cone; from there poleward the upper loss cone is filled up, suggesting that the particle distribution is in strong pitch angle scattering. The α/p ratio in the maximum of the precipitation ($L = 2.71$) is $\sim 8 \times 10^{-3}$, 2.1×10^{-3} , and 5.8×10^{-4} at 0.4, 0.5, and 0.6 MeV/nucleon, respectively. Figure 5 shows detailed pitch angle distributions of protons and alpha particles at the equatorial edge of the precipitation region. The transition from rounded (peaked at 90° to the geomagnetic field) pitch angle distributions to flat (filled upper loss cone) distributions occurs at $L = 2.59$. The higher energy protons (p4) and alpha particles ($\alpha 3$) show filled loss cones,

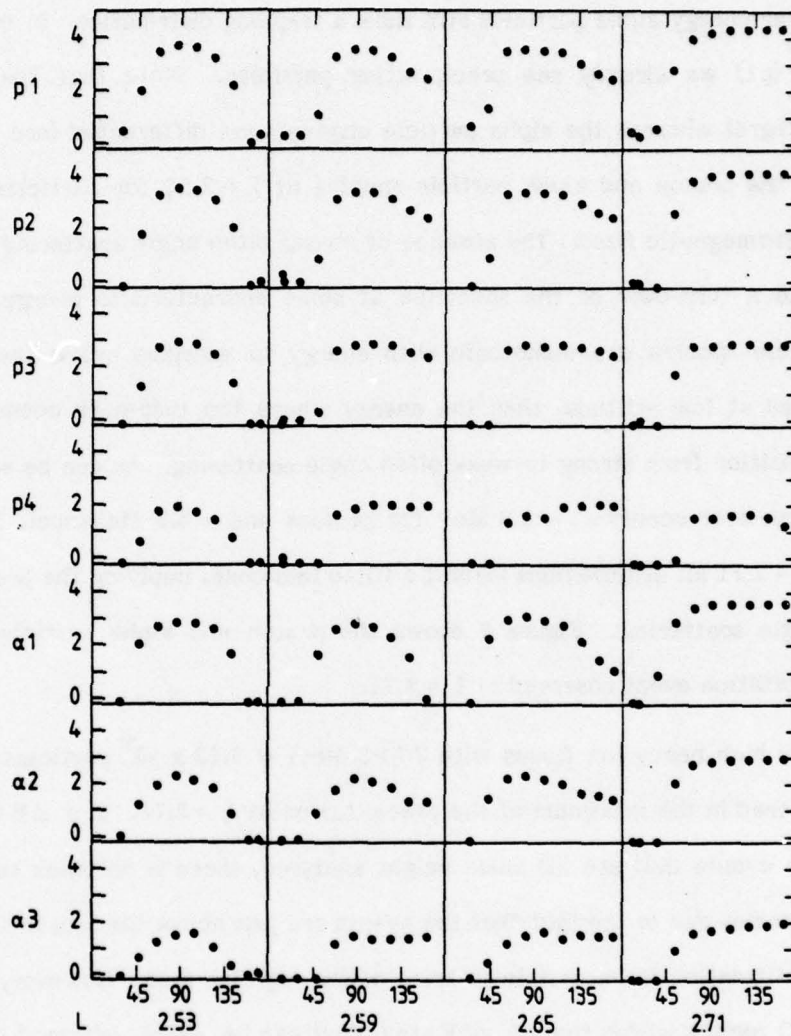


Fig. 5. Pitch Angle Distributions of Protons and Alpha Particles on 26 March 1976. Each individual plot shows \log_{10} integral count rate (for protons) or \log_{10} differential count rate (for alpha particles) versus local pitch angle for a specific energy and L value.

whereas the lower energy alpha particles still show a trapping distribution. In the lowest proton channel (p1) we already see precipitating particles. Note that the protons channels are integral whereas the alpha particle channels are differential (see Table 1). Figure 6 shows the proton and alpha particle spectra at $L = 2.59$ for particles moving parallel to the geomagnetic field. The absence of strong pitch angle scattering at lower energies leads to a turn-over of the spectrum at some characteristic energy. If the equatorial particle spectra are monotonic with energy to energies below that of the turnover observed at low altitude, then the energy where the turn-over occurs should indicate the transition from strong to weak pitch angle scattering. As can be seen from Figure 6, the turn-over occurs at ~ 2.0 MeV for protons and ~ 0.5 MeV/nuc. for alpha particles. At $L = 2.71$ all distributions exhibit a filled loss cone, implying the presence of strong pitch angle scattering. Figure 7 shows the proton and alpha particle spectra during the precipitation event observed at $L = 2.71$.

Extremely high heavy ion fluxes with $J(>3 \text{ MeV}) = 5.23 \times 10^2$ particles/cm² sec are encountered in the maximum of the precipitation at $L = 2.71$. In a ΔE vs E plot of the heavy ion events that are 2D pulse height analysed, there is no track separation into individual species due to the fact that the events are just above the sensor threshold. Thus an ion identification is impossible in spite of the high ion rate. However, the ions fall into the CNO regime within the ΔE vs E area, so it can be safely assumed that they belong to the CNO group. This heavy ion channel responds to the integral flux of CNO nuclei above 250 keV/nucleon. Integration of the alpha particle spectrum (Figure 7) above 250 keV/nucleon gives a CNO/ α ratio of $\sim 6.5 \times 10^{-2}$.

In the high latitude precipitation regions ($L \approx 3.8$) during the main phase, we derive α/p of $\sim 9.1 \times 10^{-4}$ and 2.1×10^{-4} at 0.4 and 0.5 MeV/nucleon, respectively.

TABLE 1

SENSOR PARAMETERS						
Proton telescope ($g = 0.04 \text{ cm}^2 \text{ ster}$)		Ion telescope ($g = 0.52 \text{ cm}^2 \text{ ster}$)				
Channel	Energy (MeV)	Channel	Particles	Energy (MeV)	Energy (MeV/nucleon)	
p1	0.40	$\alpha 1$	alphas	0.95 - 1.42	0.237 - 0.355	
p2	0.55	$\alpha 2$	"	1.42 - 2.03	0.355 - 0.508	
p3	1.00	$\alpha 3$	"	2.03 - 2.89	0.508 - 0.722	
p4	2.00	$\alpha 4$	"	2.89 - 4.75	0.722 - 1.19	
p5	5.11	$\alpha 5$	"	4.75 - 7.33	1.19 - 1.83	
$\alpha 0$	9.66	$\alpha 6$	"	7.33 - 24	1.83 - 6.0	
		h1	$Z > 4$		>.250	
		h2	$Z > 16$	>12.0		
		pi1	protons	0.48 - 0.76		
		pi2	"	0.76 - 1.43		

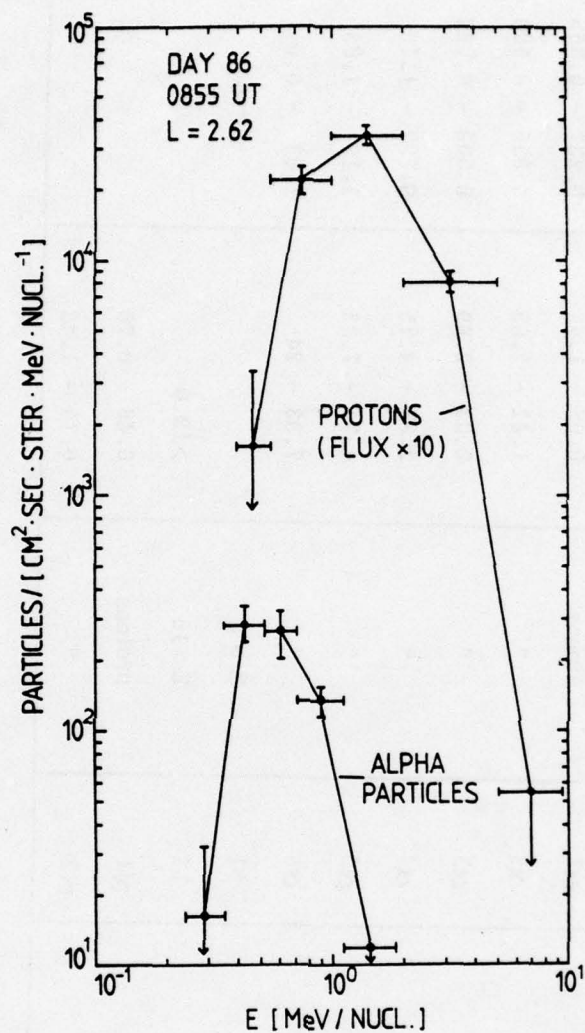


Fig. 6. Proton and Alpha Particle Differential Spectra Parallel to the Magnetic Field (upward) at L = 2.59 on 26 March 1976 at 0855 UT

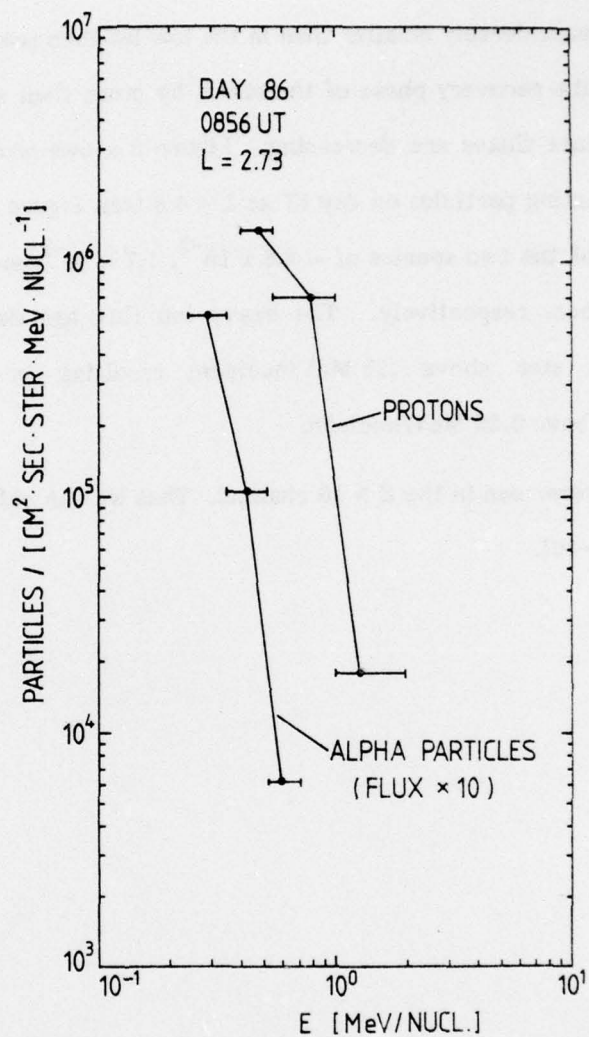


Fig. 7. Proton and Alpha Particle Differential Spectra in the Precipitation Event at L = 2.7 on 26 March 1976 at 0856 UT

Thus, the ratio is considerably smaller than in the low latitude precipitation region. This ratio increases in the recovery phase of the storm by more than an order of magnitude, although the absolute fluxes are decreasing. Figure 8 shows proton and alpha particle spectra of precipitating particles on day 87 at $L = 4.8$ (see Figure 4). From Figure 7 we derive flux ratios of the two species of $\sim 4.6 \times 10^{-2}$, 1.7×10^{-2} and 6.7×10^{-3} at 0.4, 0.5 and 0.6 MeV/nucleon, respectively. The heavy ion flux has decreased to 2.3 ± 0.94 particles/cm² sec ster above .25 MeV/nucleon, resulting in a CNO/ α ratio of $(1.1 \pm 0.5) \times 10^{-2}$ above 0.25 MeV/nucleon.

No events were seen in the $Z > 16$ channel. Thus we can only set an upper limit of 0.5% for CNO/($Z > 16$).

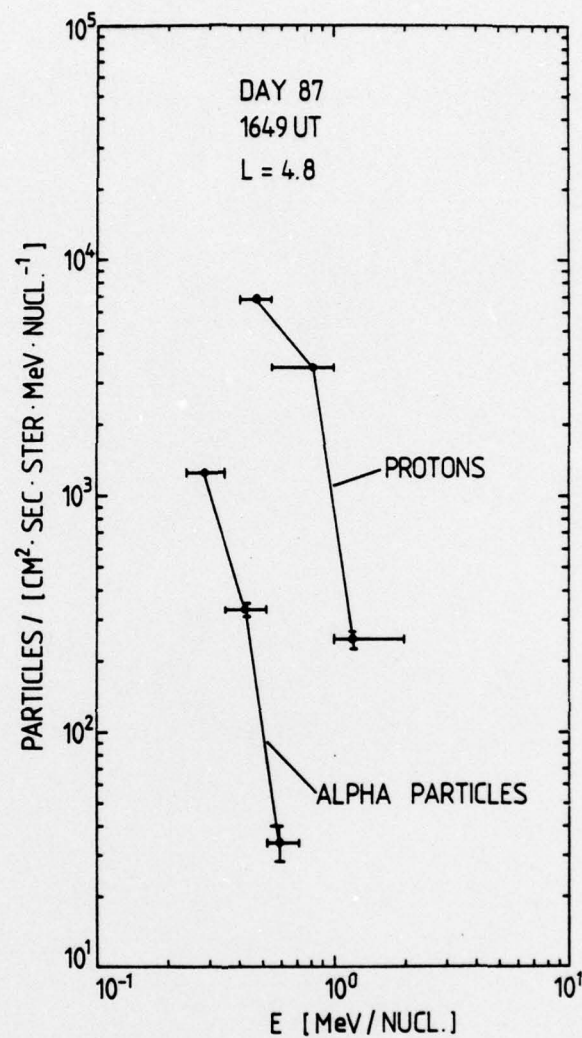


Fig. 8. Proton and Alpha Particle Differential Spectra in the High Latitude Precipitation Zone at L = 4.8 on 26 March 1976 at 1649 UT

SUMMARY OF OBSERVATIONS

The low-altitude data presented in this report can be summarized as follows:

1. Precipitating protons, alpha particles, and heavy ions have been observed during the storm main phase down to L values of ≈ 2.7 at the night side. The pitch angle distributions are isotropic except for the downward loss cone, implying the existence of strong wave turbulence down to very low L values.
2. The transition from the isotropic to the rounded pitch angle distributions occurs at an L value that decreases with increasing proton and alpha particle energy. At the time the precipitation is seen at the lowest latitudes, at $L = 2.6$, ~ 0.6 MeV/nucleon particles are in strong pitch angle diffusion while 0.3 MeV/nucleon particles are only weakly scattered. The transition from strong to weak scattering occurs at about the same total energy for protons and alpha particles.
3. A two zone night side precipitation pattern exists during the storm main phase, with a maximum at $L \approx 2.7$ and a second broad maximum at higher latitudes ($L \approx 4$). The α/p ratio is $\sim 8 \times 10^{-3}$ in the equatorward region and $\sim 9 \times 10^{-4}$ in the high latitude precipitation zone at 0.4 MeV/nucleon. Precipitating heavy ions of energies $> .25$ MeV/nucleon, presumably CNO nuclei, are found in the lower latitude precipitation zone. A CNO/ α ratio of $\sim 6.5 \times 10^{-2}$ above ≈ 0.25 MeV/nucleon is derived.

4. The low latitude precipitation zone disappears in the storm recovery phase. The α/p ratio in the high latitude zone considerably increases during the recovery phase with values up to $\sim 5 \times 10^{-2}$ at 0.4 MeV/nucleon, and a CNO/ α ratio of $\sim 1.1 \times 10^{-2}$ above 0.25 MeV/nucleon has been found.

5. No counts were seen in the $Z > 16$ channel, giving an upper limit of 0.5% for CNO/($Z > 16$) actually ($Z > 4$)/($Z > 16$) at ≈ 0.25 MeV/nucleon.

DISCUSSION

The energy dependence of the low altitude equatorial boundary of the precipitation region has been previously described by Mizera (1974) and S  raas and Berg (1974) for protons. The relation of the equatorward extension of the strong precipitation to D_{st} has been found by Mizera (1974) and by Hauge and S  raas (1975). Williams and Lyons (1974b) report equatorial pitch angle measurements of protons from which they also conclude that the outer region of strong turbulence penetrates closer to the earth during the storm main phase than during the recovery phase. S  raas and Berg (1975) propose that the proton precipitation is caused by self-excited ion cyclotron waves. In this case the condition for resonance with a growing wave is

$$E_p > E_M A^{-2} (1 + A)^{-1} \quad (1)$$

where E_p is the energy of the resonant protons, $E_M = B^2/8\pi N$ is the magnetic energy per particle, B is the magnetic field strength, N is the total plasma density and A is a measure of the proton pitch angle anisotropy. Since E_M decreases sharply with decreasing L at the plasmopause, proton precipitation by self-excited ion cyclotron waves would explain the energy dependence of the equatorward precipitation boundary. The equatorward precipitation zone should not be confused with the high latitude strong precipitation zone. The latter exists also during magnetic quiet times, and only a weak energy dependence of the low latitude boundary between one and several hundred keV (S  raas et al., 1977) has been observed there.

Let us now assume that the strong pitch angle scattering is due to a resonant interaction with electromagnetic waves. Whether these waves are self-generated by the protons or the interaction is parasitic, the resonance condition (see, e.g., Kennel and Petschek, 1966) reads

$$v_{\parallel} = v_{ph} [1 - (\Omega^+/\omega)] \quad (2)$$

where v_{\parallel} is the component of the particle velocity parallel to the magnetic field, v_{ph} is the phase velocity of the waves causing pitch angle scattering, Ω^+ is the particle gyrofrequency and $\omega/2\pi$ is the wave frequency. In the low frequency approximation the phase velocity is the Alfvén velocity v_A and the resonance frequency is

$$f = \omega/2 = \Omega^+ v_A / 2\pi v_{\parallel} \quad (3)$$

Since the gyrofrequency of protons and alpha particles differs by a factor 2, the resonance frequency for particles of the same total energy is equal. In the case of Alfvén waves propagating parallel to the magnetic field the pitch angle diffusion coefficient is given (e.g., Hasselmann and Wibberenz, 1968) by

$$D_{\mu\mu} = \frac{1}{8} \left(\frac{\Omega^+}{B}\right)^2 \frac{v_A}{v_{\parallel}} \left(\frac{1-\mu^2}{\mu}\right) P(f) \quad (4)$$

where μ is the cosine of the pitch angle and $P(f)$ is the power spectrum of the waves at the resonant frequency. This implies that the diffusion coefficient of alpha particles is

half the diffusion coefficient of protons at the same energy. The minimal condition for strong scattering is

$$D_{\mu\mu} \text{ (strong)} \geq 2 \alpha_L^2 / \tau_B \quad (5)$$

where α_L is the equatorial loss cone and τ_B is the bounce period. Since the bounce period is inversely proportional to velocity we have finally the result that if protons of a certain energy are in strong pitch angle diffusion, then the same is true for alpha particles of the same total energy and vice versa. This discussion is valid for the case of stripped helium ions, i.e., He^{++} . The radiation belt helium ions are expected to be both singly ionized and doubly ionized (Cornwall, 1972; Spjeldvik and Fritz, 1978a). What has been said above of H^+ and He^{++} is equally true of He^+ at 1/4 of the energy. Heavier ions, CNO ions in particular, will not be totally stripped in the energy range of ≈ 0.25 MeV/nucleon (Spjeldvik and Fritz, 1978b). Thus the value of e/m for the CNO ions will be $< 1/2$ and they will be in strong pitch angle diffusion at energies below that of He^{++} and H^+ . As can be seen from Figure 7, the turn-over in the spectra, i.e., the lowest energy where particles are still in strong diffusion, is at about the same energy for protons and alpha particles but the change in slope of the alpha particle spectrum is less than that of the proton spectrum. This result would be expected if the helium ions are a mixture of He^+ and He^{++} and there are significant abundances of both ionization states.

We have interpreted the isotropic distributions as being due to strong pitch angle diffusion. If the pitch angle diffusion process occurs in the near equatorial region, the ratios of different species should be characteristic of equatorial ratios. The α/p ratios of equatorially mirroring particles have been reported by Blake et al. (1973) and Fennell

and Blake (1976) for $L \leq 2.5$ and by Fritz and Williams (1973) for larger L values. At $L = 3$ Fritz and Williams (1973) observed a ratio of $\sim 8 \times 10^{-3}$, which compares favorably well with our ratio measured at $L = 2.7$ at the end of the main phase. The ratio of $\sim 10^{-3}$ at $L = 4$ during the storm main phase is low compared with a ratio of $\sim 10^{-2}$ given by Fritz and Williams; however, during the storm recovery phase our ratio increases up to $\sim 5 \times 10^{-2}$. Large increases of the α/p ratio at low altitudes coincident with geomagnetic disturbances have been observed (Van Allen and Randall, 1971; Krimigis and Verzariu, 1973; Randall, 1973). If our interpretation of the precipitation events as being due to near-equatorial strong scattering is correct, the α/p ratio near the equator also can show large variations. Large variations at low altitudes thus are not necessarily the result of relative changes of the pitch angle scattering strength for protons and alpha particles.

The first measurements of magnetospheric ions heavier than alpha particles were made by Krimigis et al. (1970) and Van Allen et al. (1970). From these low altitude measurements they derived (in the range $3.0 \leq L \leq 3.5$, $0.15 \leq B \leq 0.2$) a ratio of CNO/α of $\sim 3 \times 10^{-3}$ above ≈ 0.3 MeV/nucleon. Our measurements at the end of the storm main phase at $L = 2.7$ result in a CNO/α ratio above ≈ 0.25 MeV/nucleon which is about one order of magnitude higher. Interpreting the ratio in the precipitation event as characteristic of the near equatorially mirroring particles, we would expect a higher CNO/α ratio at large equatorial pitch angles than at small equatorial pitch angles during quiet conditions. Fritz and Wilken (1976) observed at the geostationary orbit an injection of heavy ions during an isolated substorm with a $(Z > 2)/\alpha$ ratio of $\sim 1.2 \times 10^{-1}$ at 0.15-0.23 MeV/nucleon; thus the equatorial CNO/α ratio may well be time dependent. A definite conclusion about the origin of the heavy particles is not possible since the ratio of number densities of CNO to He is similar in the solar wind (Bame et al., 1975) and in the ionosphere (Taylor, 1973), as is also the H to He ratio. A conclusive test would be the measurement of the C to O ratio (Blake, 1973).

REFERENCES

- Amundsen, R., F. Søråas, H. R. Lindalen, and K. Aarsnes, Pitch angle distributions of 100 - 300 keV protons measured by the Esro IB satellite, J. Geophys. Res., 77, 556, 1972.
- Bame, S. J., J. R. Asbridge, W. C. Feldman, and M. D. Montgomery, Solar wind heavy ion abundances, Solar Phys., 43, 463, 1975.
- Blake, J. B., J. F. Fennell, M. Schulz and G. A. Paulikas, Geomagnetically trapped alpha particles 2. The inner zone, J. Geophys. Res., 78, 5498, 1973.
- Blake, J. B., Experimental test to determine the origin of geomagnetically trapped radiation, J. Geophys. Res., 78, 5822, 1973.
- Cornwall, J. M., Radial diffusion of ionized helium and protons: A probe for magnetospheric dynamics, J. Geophys. Res., 77, 1956, 1972.
- Fennell, J. F. and J. B. Blake, Geomagnetically trapped alpha particles in Magnetospheric Particles and Fields, ed. B. M. McCormack, p. 149, D. Reidel, Dordrecht, Netherlands, 1976.
- Fritz, T. A., Ion composition, in Proc. Intern. Symp. Solar-Terrestrial Physics, ed. D. J. Williams, p. 716, American Geophysical Union, 1976.

- Fritz, T. A. and B. Wilken, Substorm generated fluxes of heavy ions at the geostationary orbit, in Magnetospheric Particles and Fields, ed. B. M. McCormack, p. 171, D. Reidel Dordrecht, Netherlands, 1976.
- Fritz, T. A. and D. J. Williams, Initial observations of geomagnetically trapped alpha particles at the equator, J. Geophys. Res., **78**, 4719, 1973.
- Hasselmann, K. and G. Wibberenz, Scattering of charged particles by random electromagnetic fields, Z. Geophys., **34**, 353, 1968.
- Hauge, R. and F. Søråas, Precipitation of >115 keV protons in the evening and forenoon sectors in relation to the magnetic activity, Planet. Space Sci., **23**, 1141, 1975.
- Hovestadt, D. and O. Vollmer, Satellite experiment for detecting low energy heavy cosmic rays, in Proc. Cosmic Ray Conference, **4**, p. 1608, Hobart, Tasmania, 1971.
- Kennel, C. F. and H. E. Petschek, Limit on stably trapped particle fluxes, J. Geophys. Res., **71**, 1, 1966.
- Krimigis, S. M., P. Verzariu, J. A. Van Allen, T. P. Armstrong, T. A. Fritz, and B. A. Randall, Trapped energetic nuclei $z > 3$ in the earth's outer radiation zone, J. Geophys. Res., **75**, 4210, 1970.
- Krimigis, S. M. and P. Verzariu, Measurements of geomagnetically trapped alpha particles, 1968 - 1970. 1. Quiet time distributions, J. Geophys. Res., **78**, 7275, 1973.

Lindalen, H. R. and Å. Egeland, Observations of trapped and precipitated protons on March 8, 1970, Ann. Geophys., 28, 129, 1972.

Mizera, P. F., Observations of precipitating protons with ring current energies, J. Geophys. Res., 79, 581, 1974.

Randall, B. A., Time variations of magnetospheric intensities of outer zone protons, alpha particles, and ions ($z > 2$), Univ. of Iowa Res. Rept., 73.3, 1973.

Søråas, F., J. A. Lundblad, and B. Hultquist, On the energy dependence of the ring current proton precipitation, Planet. Space Sci., 25, 757, 1977.

Spjeldvik, W. N. and T. A. Fritz, Energetic ionized helium in the quiet time radiation belts: Theory and comparison with observation, J. Geophys. Res., 83, 654, 1978.

Spjeldvik, W. N. and T. A. Fritz, Theory for charge states of energetic oxygen ions in the earth's radiation belts, J. Geophys. Res., in press, 1978.

Taylor, H. A., Jr., Parametric description of thermospheric ion composition results, J. Geophys. Res., 78, 315, 1973.

Van Allen, J. A., B. A. Randall, and S. M. Krimigis, Energetic carbon, nitrogen, and oxygen nuclei in the earth's outer radiation zone, J. Geophys. Res., 75, 6085, 1970.

Van Allen, J. A. and B. A. Randall, Evidence for direct durable capture of 1- to 8- MeV solar alpha particles onto geomagnetically trapped orbits, J. Geophys. Res., 76, 1830, 1971.

Williams, D. J. and L. R. Lyons, The proton ring current and its interaction with the plasmopause: Storm recovery phase, J. Geophys. Res., 79, 4195, 1974a.

Williams, D. J. and L. R. Lyons, Further aspects of the proton ring current interaction with the plasmopause: Main and recovery phases, J. Geophys. Res., 79, 4791, 1974b.

THE IVAN A. GETTING LABORATORIES

The Laboratory Operations of The Aerospace Corporation is conducting experimental and theoretical investigations necessary for the evaluation and application of scientific advances to new military concepts and systems. Versatility and flexibility have been developed to a high degree by the laboratory personnel in dealing with the many problems encountered in the nation's rapidly developing space and missile systems. Expertise in the latest scientific developments is vital to the accomplishment of tasks related to these problems. The laboratories that contribute to this research are:

Aerophysics Laboratory: Launch and reentry aerodynamics, heat transfer, reentry physics, chemical kinetics, structural mechanics, flight dynamics, atmospheric pollution, and high-power gas lasers.

Chemistry and Physics Laboratory: Atmospheric reactions and atmospheric optics, chemical reactions in polluted atmospheres, chemical reactions of excited species in rocket plumes, chemical thermodynamics, plasma and laser-induced reactions, laser chemistry, propulsion chemistry, space vacuum and radiation effects on materials, lubrication and surface phenomena, photo-sensitive materials and sensors, high precision laser ranging, and the application of physics and chemistry to problems of law enforcement and biomedicine.

Electronics Research Laboratory: Electromagnetic theory, devices, and propagation phenomena, including plasma electromagnetics; quantum electronics, lasers, and electro-optics; communication sciences, applied electronics, semiconducting, superconducting, and crystal device physics, optical and acoustical imaging; atmospheric pollution; millimeter wave and far-infrared technology.

Materials Sciences Laboratory: Development of new materials; metal matrix composites and new forms of carbon; test and evaluation of graphite and ceramics in reentry; spacecraft materials and electronic components in nuclear weapons environment; application of fracture mechanics to stress corrosion and fatigue-induced fractures in structural metals.

Space Sciences Laboratory: Atmospheric and ionospheric physics, radiation from the atmosphere, density and composition of the atmosphere, aurorae and airglow; magnetospheric physics, cosmic rays, generation and propagation of plasma waves in the magnetosphere; solar physics, studies of solar magnetic fields; space astronomy, x-ray astronomy; the effects of nuclear explosions, magnetic storms, and solar activity on the earth's atmosphere, ionosphere, and magnetosphere; the effects of optical, electromagnetic, and particulate radiations in space on space systems.

THE AEROSPACE CORPORATION
El Segundo, California
. . .